THE SIMULATION OF THE GEOSYNCHRONOUS EARTH ORBIT PLASMA ENVIRONMENT IN CHAMBER A; AN ASSESSMENT OF POSSIBLE EXPERIMENTAL INVESTIGATIONS

BY NASA CR-160997

William Bernstein

Center for Space Physics

Dept. of Space Physics & Astronomy

Rice University, Houston, TX 77001

A Final Report of the

Research on NASA Contract NAS9-16166

January 1981

Introduction and Summary

This report considers the possible use of Chamber A for the replication or simulation of space plasma physics processes which occur in the Geosynchronous earth orbit (GEO) environment. It is shown that replication is not possible and that scaling of the environmental conditions is required for study of the of the important instability processes. Rules for such experimental scaling are given. At the present time, it does not appear technologically feasible to satisfy these requirements in Chamber A.

It is, however, possible to study and qualitatively evaluate the problem of vehicle charging at GEO. In particular, Chamber A is sufficiently large that a complete operational spacecraft could be irradiated by beams and charged to high potentials. Such testing would contribute to the assessment of the operational malfunctions expected at GEO and their possible correction. However, because of the many tabulated limitations in such a testing programs, its direct relevance to conditions expected in the GEO environment remains questionable.

Philosophy of Simulation Experiments

Block (1976) has succinctly summarized both the relevance and limitations of laboratory experiments in the space plasma physics area as follows:

a) New theories should as far as possible be tested in laboratory.

b) Theoretical processes which cannot or have not been reproduced in the laboratory should often be met with scepticism when applied to space plasmas.

c) Most plasma processes observed in the laboratory are probably of importance in space.

d) Proper application of a laboratory process to space conditions requires a theoretical understanding of its dependence on all plasma parameters and boundary conditions.

These rules may seem self-evident, but they are unfortunately not always obeyed, since too many theoreticians are not aware of the multitude of plasma phenomena not understood theoretically, and too many experimentalists are unaware of appropriate theories. There is of course at least a partial excuse: paper proliferation.

Because of the immensity of space plasma configurations, scaling must be applied to reduce the experiment size such that it can be accomodated in a laboratory system. Block [1976] also gives a quantitative tabulation of the the various scaling dependences shown in Table I.

Length, time, resistivity	vary as L^{+1}
Particle energy, velocity, potential, temperature	vary as L^{0}
Particle density and pressure, electric and magnetic field, frequency	vary as L^{-1}
Magnetic pressure, space charge density, current density	vary as L^{-2}

Table 1. Plasma Scaling Laws

It seems reasonably clear that, in most instances, quantitative scaling will not allow technologically feasible laboratory configurations; therefore the concept of qualitative, limited scaling has been introduced. This means that the relevant dimensionless numbers [such as the ratio of the electron-neutral collision frequency to the electron cyclotron frequency] should be kept qualitatively the same in the laboratory as in space. Ratios much smaller or larger than unity retain this property but not necessarily the same order of magnitude. Problems of course remain with ratios that are near unity.

In some cases, the need for even qualitative scaling can be relaxed still further and idealized geometrical configurations and idealized particle distribution functions can be employed in the laboratory experiments. The objective here is the test of theoretical concepts: the experimental conditions need only satisfy the constraints of the specific theory, not duplicate the

total complex set of phenomena. The direct relevance of the specific theory under study to space plasma physics phenomena cannot be established by the laboratory experiments alone.

The use of a very large experiment system offers several important advantages.

1. The range of the parameter scaling is reduced, and therefore the uncertainties associated with dimensionless ratios near unity are reduced. In fact, the existing work that has been performed in Chamber A has been performed under conditions where only minor scaling has been required. It should be noted, however, that only extremely small scale local phenomena have been studied in the configuration. The study of longer range phenomena (several meters) would obviously require at least qualitative scaling.

2. Operation at smaller magnetic field strengths and particle densities reduce the pertinent electron plasma and cyclotron frequencies to a very convenient range.

3. The temporal evolution of plasma phenomena is slowed.

4. Insertion of various diagnostics into the plasma is possible without severe perturbations, which modify the properties under study.

The utility of scaling experiments is clearly shown in the work of Bernstein et al. (1979) describing the Beam Plasma Discharge. These experiments represented an inverse scaling, in which phenomena first observed in small laboratory configurations were demonstrated to occur for the large dimensions available in space experiments. They noted that the critical beam current for ignition scaled quantitively with earlier work in the small laboratory systems despite the very large change in parameters ($\frac{B_o}{B_I} = 10^3$, $N_{eo}/N_{e_I} \approx 10^4$, $L_o/L_I = 0.02$). where I represents near ionosphere conditions. Although Soviet investigators did not produce the BPD under laboratory condi-

tions approximating the ionosphere, they independently interpreted the confusing results of several electron gun rocket flights in terms of the BPD.

In this report we will first summarize the plasma characteristics existing at GEO and then determine whether it is possible to perform meaningful laboratory experiments relevant to processes occurring at GEO.

Plasma Characteristics at GEO

Fig. 1 is an overly complex schematic representation of the magnetosphere taken from DeForest (1978). The location of GEO at all local times is indicated. Obviously, GEO lies in a fixed geographical position with respect to the Earth, but all the illustrated plasma boundaries show large temporal variations in radial location not only in assocation with diurnal and seasonal effects, but transiently with the level of geomagnetic activity. Thus sometimes GEO may be located within the high density, co-rotating plasmasphere, the ring current-plasma sheet region, and even, during severe geomagnetic storms, within the unperturbed solar wind beyond the bow shock. Fig. 2, given by Bernstein et al. (1974) shows the correlated dependence of the plasmapause (the boundary between the co-rotating plasmasphere and the ring current region) and the equatorial boundary of isotropic ion precipitation on geomagnetic activity characterized by the Kp index. Thus for quiet conditions, GEO (L-6.6) lies partially within the plasmasphere; for more active conditions, GEO lies entirely within the ring current region.

Chappell (1972) has given a comprehensive report on the distribution of cold plasma (T_e < 10 eV) within the magnetosphere. Within the plasmapause, the dependence of plasma density on radial distance varies as R^{-4}. The plasmapause boundary is characterized by an abrupt drop (1-2 orders of magnitude) decrease in plasma density; beyond the plasmapause this cold density typically

varies from 0.1 - 1 cm^{-3}. As represented in Fig. 1, the plasmapause is circular in shape; a more detailed representation is shown in Fig. 3 showing a pronounced outward bulge in its location in the dusk sector (Chappell, 1972). Mass spectrometric measurements indicate the dominant ion to be H^+ with some He^+ present within the plasmapause. At times localized regions of high cold plasma density (detached) are observed outside the plasmapause.

The region outside the plasmapause is populated by a low density, hot plasma. Garrett (1979) has tabulated the hot plasma characteristics in this region; the measurements considered were conducted predominantly from geosynchronous spacecraft. Typically, electron temperatures (based on the assumption of a Maxwellian velocity distribution) are in the range of a few KeV; ion temperatures are ~ 20 KeV. Typical hot plasma densities lie in the range of 1-2 cm^{-3}; thus the ratio N_e/N_H can be as small as 0.1. As might be expected, the assumed maxwellian distributions represent only a qualitative approximation; careful comparison indicates the presence of non-Maxwellian distributions. Large (order of magnitude) variations in density together with smaller variations in temperatures occur. The ion composition is highly variable; at times H^+ or O^+ may be the dominant ion; both He^{++} and He^+ are also observed but usually not as the dominant ion. The presence of He^+ and O^+ (higher charge states of O have not been observed) ions indicate an ionospheric origin; He^{++} ions are attributed to a solar wind source. Thus the hot plasma population originates from both the solar wind and ionosphere with large temporal variations in the respective abundances.

The particle angular distributions are not completely isotropic. Because of the mirror magnetic field geometry, particles with large $v_\parallel/v_\perp$ relative to the magnetic field are preferentially lost to the atmosphere (within the loss cone) ~ $\pm$ 6° at GEO. Williams and Lyons (1974) report that during the

recovery phase of large geomagnetic storms, the ion population in the region extending 1-2 R_e beyond the plasmapause may show a totally depleted loss cone for ions. The empty loss cone indicates the absence of pitch angle scattering processes. At large L, the ring current does, in fact, show a completely isotropic pitch angle distribution (full loss cone). This isotropy for energetic electrons and ions is evidence for the occurrence of strong pitch angle scattering which almost surely results from a variety of plasma instabilities (the electromagnetic ion cyclotron (Cornwall et al., 1970), electromagnetic electron cyclotron (Kennel and Petschek, 1966), and electrostatic electron cyclotron (Kennel et al., 1970) instabilities. It appears likely that electrostatic ion cyclotron modes are important at large L, but experimental verification is lacking (Bernstein et al., 1974). These particle losses to the atmosphere are the origin of the diffuse aurora and provide a mechanism which limits the energetic particle population in the outer magnetosphere. Conversely, McIlwain (1975) has reported transient observations of KeV field aligned (within the loss cone) electron and ion beams at GEO. Thus the angular pitch angle distribution can range from $\frac{v_\perp}{v_\parallel} > 1$ to isotropy to $\frac{v_\perp}{v_\parallel} < 1$. Auroral arcs cannot be mapped to the equatorial plane on the auroral field lines. General conclusions are that the arcs are generated in field aligned accelerating regions located in the vicinity of 1-3 Re. The equatorial plane ion beams may be associated with this acceleration, however.

Other important parameters at GEO include the solar UV flux together with transient periods of eclipse and the dipole (mirror) magnetic field configuration. The field strength at GEO is typically $100 \pm 50 \times 10^{-5}$ gauss. Typically, the hot plasma region is characterized by large β where $\beta = \frac{8\pi N\ KT}{B^2} \approx 0.25$. We note again that GEO can lie beyond the magnetosphere (at the sub-solar point) so that the vehicle is immersed in the solar wind (DeForrest, 1973).

TABLE 2. Estimates of Minimum, Typical, and Maximum Values for the First Four Moments of the Distribution Function [*DeForest and McIlwain*, 1971] as a Function of Local Time

	Electrons						Protons					
	0000	0300	0600	1200	1800	2100	0000	0300	0600	1200	1800	2100
						Number Density, Particles cm^{-3}						
Minimum	0.07	0.22	0.17	0.06	0.02	0.04	0.7	0.6	0.7	0.3	0.5	0.6
Maximum	8.3	4.8	2.9	1.2	1.9	4.4	3.8	3.5	1.9	2.2	2.2	2.4
Typical	2.0	2.0	1.2	0.4	0.10	0.4	1.2	1.2	1.2	0.9	0.8	1.1
						Energy Flux, erg cm^{-2} s^{-1} sr^{-1}						
Minimum	0.21	0.38	0.42	0.26	0.04	0.10	0.16	0.13	0.05	0.13	0.14	0.14
Maximum	9.4	15.2	14.6	2.3	1.01	7.2	0.61	0.47	0.47	0.76	0.63	0.85
Typical	3.0	3.0	1.5	1.0	0.40	0.5	0.3	0.3	0.3	0.22	0.30	0.30
						Number Flux, 10^{8} Particles cm^{-2} s^{-1} sr^{-1}						
Minimum	15	37	32	15	2	9	6	4	4	2	4	5
Maximum	1510	1020	832	122	162	864	25	17	16	15	23	25
Typical	300	300	200	70	30	60	12	10	8	7	8	10
						Pressure, 10^{-10} dyn cm^{-2}						
Minimum	2.7	6	6	4	0.4	1	66	51	25	31	54	56
Maximum	190	266	173	25	14	128	235	196	169	242	255	327
Typical	50	60	30	12	7	8	140	120	90	80	90	120

Data, from ATS 5, are for the energy range 50 eV to 50 keV and 1970.

Table II, from Garrett (1979), shows some of the wide range of plasma conditions encountered at GEO. Note that this table is limited to particles with E > 50 eV. Thus the cold plasma component is omitted. Because the plasmapause also represents the equatorial boundary of the hot component, the simultaneous occurrence of large cold plasma densities together with the hot component is unlikely except within a localized boundary region. Superimposed on the diurnal variations are the even larger variations associated with geomagnetic activity.

The important plasma instabilities are basically characteristic of the hot plasma component. In general, the free energy source lies in the pitch angle anisotropy arising from the presence of finite loss cones. The end result of the instabilities is the establishment of an isotropic pitch angle distribution; however, because of particle loss, complete isotropy may not be realized and the instabilities may persist in steady state. On the other

hand, the instabilities may, in fact, be transient at a fast enough occurrence frequency so that they appear steady state in the measurements.

The occurrence of the instabilities depends critically upon the total plasma density (hot and cold components) although large cold plasma densities, such as exist within the plasmapause, quench instability growth. It is for this reason, that the density gradient at the plasmapause has been postulated to be a likely region of ion cyclotron wave growth (Cornwall et al., 1970) Unfortunately, although certain features of the ion pitch angle distribution are indeed consistent with the occurrence of this mode, the close asociation of ion cyclotron waves with changes in the pitch angle distribution has not been well established. A particularly interesting active experiment (Project Firewheel--this payload was launched in Spring 1980 but failed due to vehicle malfunction) attempts to destabilize the hot ion and electron components near GEO through the artificial increase in cold plasma density produced by large chemical releases. The present space measurements have not conclusively established the required close association between waves and particle energy and angular distributions inherent in the theoretical treatments. If these instabilities could be successfully studied in a laboratory configuration, confidence in the applicability of the theoretical treatments to space processes would be greatly improved.

A second consequence of the presence of hot plasma coupled with the absence of cold plasma is the charging of GEO Spacecraft to high potentials. Charging itself leads to the gross distortion of some scientific measurements, particularly those of the characteristics of the low to moderate energy plasma. In fact, several techniques to reduce charging potential have been proposed and tested in space. Unfortunately these techniques lead, in turn, to the distortion of other ambient measurements, particularly plasma waves and

consequently have not been employed on scientific missions where charging is anticipated such as Galileo (Jupiter Orbiter). Of greater operational significance is the occurrence of arcs from one point of the vehicle to another or to the plasma. The large transient currents in the spacecraft structure arising from these arcs represent a source of intense electromagnetic interference and may even produce component failures. Their occurrence has been clearly demonstrated to be associated with periods of high geomagnetic activity.

Charging results because an isolated, equipotential object, immersed in a plasma, assumes a potential relative to the plasma such that the net current to and from the object equals zero; $I_{to} + I_{from} = 0$.

Current away from the object [negative charge to and positive charge from the object] is produced almost entirely by the flux of ambient energetic and cold electrons impacting the object.

Current to the object [negative charge from and positive charge to the object] arises from a variety of sources including:

1) Positive ions from the plasma impacting the object. In general, unless $T_+ \gg T_e$, this flux is small compared to electron flux to the object because $v_+ = \sqrt{(m_e/M_+)}\ \bar{v}_e$.
2) Secondary electron emission + backscatter.

Energetic electrons and ions can eject low energy (< 50 eV) electrons when they strike surfaces. For most clean materials the secondary yield is < 1 although, of course, selected surfaces with yields > 1 have widespread applications. The secondary yield is energy dependent with the maximum yield for electrons occurring at ~ 200-500 eV; at higher energies, the secondary

yield decreases with increasing energy approximately as KE^{-m} (Wall et al., 1977). Similarly a fraction of the incident enegetic electron flux will be backscattered from surfaces. Wall et al. (1977) suggest the following empirical relationship for the backscatter yield, $B \sim AE^{-n}$. For both equations the quantities K, A, m, n are characteristic of the particular surface material and the angle of incidence of the primary particles.

3) Photo electron emission

Surfaces irradiated with UV and shorter wavelength light emit photoelectrons. The photoelectron yield again depends upon the surface material and the photon angle of incidence.

Both the secondary and photoelectron emission are primarily surface phenomena. In space, after prolonged exposure in the ultra-high vacuum environment coupled with energetic particle and solar photon irradation, it is likely that the surfaces will be clean with yields characteristic of the materials themselves. Under poor vacuum conditions ($> 10^{-6}$ torr) surfaces will be covered with monomolecular layers of contaminant materials; in general such contamination results in increased yields. Such layers cannot be removed by prolonged pumping alone; rather baking at > 200°C or intense energetic particle bombardment is required. Furthermore, at poor operating pressures, the layers will be rapidly redeposited once they are removed.

Because it has been assumed that the surface is an equipotential (conducting) surface, spatial non-uniformities in the distribution of charging and discharging currents do not lead to differential charging. Rather the final uniform potential distribution arises from the total charging and discharging currents.

The magnitude of the charging and discharging currents and the potential distribution are not uncoupled parameters however. This situation arises because the dimensions of the sheath surrounding the charged object increase with increasing potential. It is the dimensions of the sheath rather than that of the object itself which determine the effective area for the collection of charge neutralizing current from the ambient plasma. Secondarily, the energy angular distribution of particles striking the object surface will be modified in their transit of the sheath region with consequent modification of the secondary emission and backscatter yields. Complex computer programs have been developed (see, for example, Katz et al, 1977) for this parameter interdependence. If ion and electron gyroradii are large compared to sheath dimensions, the configuration can be treated as unmagnetized. At lower altitudes where B is greatly increased, gyroradii may be < sheath dimensions and consequently the magnetic field modifies the neutralizing current collection configuration. However, the stability of such sheath configurations for conditions where $\omega_p > \omega_c$ (typical of the ionosphere) has not been well established; the consequence of such sheath turbulence has been proposed to produce enhanced crossed field diffusion of plasma. At the present time most theoretical treatments of the neutralization at GEO do not consider magnetic field effects.

Differential charging of various regions of the object surface results if the surface is not an equipotential; that is if regions of the surface are insulators. Because of the different photoelectron, secondary electron, and backscatter yields coupled with both photon and energetic particle shadowing arising from the object geometric configuration, differential charging of various portions of the surface can be produced. Obviously the bulk conductivity of the insulating regions determines the conduction charge loss and the

magnitude of the potential differences which can be maintained. Thus the bulk conductivity represents another surface material property influencing the final potential distributions. It is these large potential differences between nearby regions which produce the vacuum arcs and both malfunction and damage of spacecraft components.

Reference to Fig. 1 indicates that this high potential phenomenon is not restricted to GEO. It can occur throughout the entire region of the magnetosphere beyond the plasmapause where the hot plasma of the ring current and plasma sheet dominate the cold plasma. Charging, of course, occurs throughout the magnetosphere; in the high density region within the plasmapause, the floating potential remains low (few volts) even in the presence of large energetic particle fluxes such as the aurora. In sunlight, photoelectron emission may dominate plasma effects and a positively charged object results. Such charging has negligible operational impact, but can severely impact measurements of the local low energy plasma characteristics.

Charging patterns also are produced when the object emits either electron or ion beams. Usually beam currents are planned to be far in excess of the maximum return (neutralizing) total current from the ambient medium even within the high density lower ionosphere. In the case of the space shuttle, the collecting surface is ~ 80% insulating tiles. It is possible that very large potential differences may be produced between different insulating areas and between these and the conducting surfaces. However, intense beams have been launched from rockets with little evidence for charging to excessive potentials. It is believed that charge neutralization is achieved through the local production of a very high density plasma surrounding the vehicle which can supply the required neutralizing current. This can be accomplished by

either the Beam-Plasma-Discharge or an E x B (Penning) discharge (Galeev et al., 1976) in which the ambient neutral gas is ionized. Success of beam experiments planned for Spacelab require such "non-classical" local sources of ionization. Other possible neutralization schemes include the use of plasma sources and the deployment of very large area collecting surfaces, none of which are planned for early flights. Measurements (Bernstein et al., 1980) with an isolated electron gun payload in Chamber A have shown that BPD ignition does neutralize beam emission currents of ~ 100 ma. Obviously, if neutralization does occur, large differential charging potentials are eliminated.

What Can Be Studied in the Large Vacuum Chamber

From the previous discussion, it is concluded that the most interesting plasma phenomena are those associated with the hot plasma region. Although conditions there are highly variable, we can assume the following to be representative: $Ne = 1\ cm^{-3}$, $Te = T_H = 10$ keV, and $B = 10^{-3}$ gauss. We therefore obtain the following important dimensions:

Debye length, $\lambda_D \approx 7 \times 10^4$ cm

Proton Gyroradius $\rho_H \approx 4.7 \times 10^6$ cm

Electron Gyroradius $\rho_e \approx 1.1 \times 10^5$ cm

Treatment of the ions and electrons as a magnetized plasma requires that these be $<<$ the dimensions of the system. Thus, even if the ambient magnetic field in the chamber could be reduced to 10^{-3} gauss, exact simulation of the GEO plasma environment is not possible. Scaling according to the rules given earlier is required.

The plasma density and magnetic field strength required to reduce the above dimension to < 10 cm for a 10 keV thermal plasma are

$$\text{Plasma density} \approx 5 \times 10^{7}\ \text{cm}^{-3}$$

$$\rho_H \approx 4.7 \times 10^{2}\ \text{gauss}$$

$$\rho_e \approx 11\ \text{gauss}$$

At the present time, I cannot identify any method of producing this plasma density at 10 keV with a loss cone angular distribution in the chamber. This is not meant to imply that scaled experiments are not possible; rather we conclude that it is not feasible to produce even the qualitative scaling conditions in Chamber A. Several laboratory experiments in small magnetic mirror confinement systems have demonstrated the occurrence of the electromagnetic electron cyclotron instability, one of the critical instabilities limiting the energetic electron population in the outer magnetosphere (Ikegami et al., 1969; Jacquinot et al., 1969).

Simulation of charging phenomena present a very different set of constraints. As noted earlier, quantitative simulation of the charging process requires quantitative duplication of all environmental and surface conditions. Even if this could be accomplished, the finite dimensions of any laboratory configuration ($R < \lambda_D$) produces gross modifications in the sheath configuration and hence the trajectories of the incident particles.

It is possible however to study the charging process in idealized experiments which do not duplicate or scale the space environment. Here the objectives are limited to the following:

1. To determine whether differential charging to large potential difference can occur.

2. To determine whether these large potential differences will produce arcs, and at what potential difference arcing will occur.
3. To identify the operational consequences of such arcing.

The use of the large chambers offers several important advantages as follows:

1. The large dimensions of the chamber allow the irradiation of larger and more complex structures than can be studied in the presently used laboratory experiments.
2. The availability of the solar simulator could allow photoelectron emission to be included as an experimental parameter. However, because the simulator does not duplicate the solar EUV spectrum (Lα and shorter wavelengths), the value of the simulation is doubtful.
3. The role of electrically grounded conducting boundaries in the breakdown process is reduced because of the greater distance from the surface to the wall.

For these qualitative studies of charging, low density energetic electron and ion beams from wall mounted accelerators, can provide a reasonable approximation of the natural energetic electron. The characteristics of these electron beams together with the techniques for electron beam generation outlined in the Spire report [1979] appear adequate. Energetic ion beams are unnecessary because vehicle charging by energetic ions in nature is unlikely. A low energy ion source would be desirable.

The poor vacuum conditions in Chamber A will provide some uncertainties in the significance of the results for the following reasons:

1. Both the secondary electron and photo electron fields are dependent on surface properties. The presence of contaminant layers modifies

the surface characteristics severely. Also the presence of such layers may modify breakdown characteristics. Cleaning by baking or prolonged electron bombardment together with ultra high vacuum techniques are usually employed to ensure clean surfaces. At pressures $> 1 \times 10^{-6}$ torr, with significant H_2O vapor partial pressures, it is questionable whether clean surfaces can be maintained after cleaning. Also bombardment cleaning may be dangerous to complex structures.

2. The passage of energetic particle beams through the residual neutral gas will produce significant ionization. The fraction of primary 10 kV electrons producing 1 ion pair in a 20M path length, L, is given by

$$\frac{L}{MFP} = \frac{L}{N_o \sigma_i} = 1\text{-}2 \times 10^{-2}$$

The ionization electrons will eventually impact the chamber walls; the ions will reach the target surface however and can modify the charge balance. At $P \approx 10^{-6}$ torr, this effect is unimportant; at 10^{-5} torr and greater, the steady state ion flux can be extremely important in modifying the charging process.

The following problems in simulation of plasma phenomena in general are apparent:

1) The electromagnetic cyclotron instabilities are characteristic of high β plasmas; at Lower β, electrostatic instabilities become dominant. Almost all laboratory plasma devices (Tokamaks, Stellarators, mirrors, etc.) currently operate in the low β ($<10^{-2}$) regime. As noted in the scaling relationships, quantities such as density and magnetic field strength scale as

L^{-1} whereas magnetic pressure scales as L^{-2}. This implies severe difficulties in the direct scaling of high B GEO plasma processes where $B_{(geo)} \approx 0.25$.

2) The magnetic field particle anisotropy configuration is difficult to simulate. The hot plasma is confined in the mirror field geometry with a mirror ratio $B_{eq}/B_M \approx \frac{1}{50}$ so that the loss cone in the equatorial plane is only a few degrees. Yet, it is the particle spatial anisotropy arising from the finite but small loss cone which provides the energy source for the instabilities. The use of a smaller mirror ratio increase the magnitude of the loss cone and in turn modifies the $v\perp/v\parallel$ ratio from that at GEO.

3) A cold plasma density slightly larger than the hot plasma density quenches most postulated GEO instabilities. Cold plasma will be produced by two processes: (a) charge exchange of energetic ions with ambient neutral gas and (b) collisional ionization of the ambient neutral gas by the energetic particles. Although the lifetimes of the hot and cold plasma components in the mirror geometry will be different, a relatively dense cold component will accumulate at large neutral gas densities.

4) No obvious techniques exist for the production of the hot plasmas/ electron and ion components in the density range $> 10^7$ equired by simple dimensional scaling within the mirror geometry.

For these reasons, it is concluded that the simulations of GEO-plasma processes do not seem possible in Chamber A within the limitation imposed by present technology. It should be noted that the EM electron cyclotron instability has been apparently produced in some experiments with fusion oriented mirror devices, but the instability characteristics have not been studied in sufficient detail to demonstrate their relevance to space plasma physics processes (Ikegami et al., 1969; Jacquinot et al., 1969).

Simulation of charging phenomena presents a very different set of circum-

stances. As noted earlier, the quantitative simulation of the charging process requires quantitative duplication of all environmental and surface conditions. Even slight deviations from exact scaling would obviate results from scaled experiments, and here quantitative simulation rather than scaling would be the preferred approach. Of course, the finite dimensions of any laboratory configuration with sheath dimensions larger than chamber dimensions produces gross modifications in the overall sheath configuration because of the grounded boundaries. The presence of grounded boundaries in near proximity allows the occurence of arcs from charged surfaces to ground; however, because the walls are reasonably removed from the object in the large chamber, and more closely spaced regions of large potential difference will be present, the simulation improves with chamber size. It seems reasonable to derive the following from a charging simulation experiment.

1) To determine whether differential charging to potential differences exceeding a few KV can occur with maximum particle energies in the range of 20-30 Kev (the range expected at GEO). These measurements do not necessarily imply the magnitude of the potential differences which will be encountered at GEO because of the limited nature of the simulation. Rather they indicate that the surface and volume conductivity characteristics are such that they will allow the existence of such large potentials.

2) To determine whether these large potential differences will produce vacuum arcs, and at least, qualitatively, the minimum potential difference at which arcing occurs.

3) To identify operational consequences of the arcing; these include component failure (infrequent) and transient operational malfunctions.

The use of the large chamber offers some major advantages in the assessment of the charging problem for large complexstructures as follows:

1) It is possible to test a large complex spacecraft; present testing procedures in small vacuum systems can only accomodate small objects and therefore a total system test is impossible. Therefore, experiments in small systems have been limited to tests of the surface and volume properties of isolated surface materials. These data are subsequently included in the large computer programs to evaluate the system charging problem.

2) The presence of the solar simulator allows for inclusions of photoemission effects in charging. However, the chamber does not adequately reproduce the space geometry so that shadowing and angle of incidence is changed.

3) The roles of electrically conducting boundaries have been discussed.

4) Complete systems can be irradiated so that operational effects can be evaluated rather than estimated.

Present approach to the charging problem

At the present time, the vehicle charging problem at GEO appears reasonably well understood. Several approaches to the problem have been attempted including

1) Ideally the use of conducting material for the spacecraft surface so that the entire surface is an equipotential. For some cases when insulator properties are required, insulating glass cloths have been developed which retain their insulating characteristics at small applied potential differences, but where conductivity increases at potential differences in the few KV range. Effectively use of such materials limits differential charging to potential differences less than the vacuum arc threshhold..

For cases where the surface is the ideal equipotential, active techniques can be employed to prevent charging of the entire vehicle to large potential differences with respect to the ambient plasma. These techniques include

field and/or thermionic electron emission sources and plasma generators. Obviously neither of these techniques will eliminate differential charging effects caused by the presence of insulating surfaces; rather only the potential of the conducting surfaces will be clamped to the plasma potential.

2) In the case of insulating surfaces, the secondary electron and photoelectron yields, together with the bulk conductivity (the conductivity may be a function of the potential difference) can be determined in laboratory experiments. Furthermore laboratory experiments also yield the threshold voltage required for vacuum arcs. These data, coupled with assumed plasmas distributions allow estimates of vulnerability of various insulating regions of a spacecraft to charging problems.

3) Inclusion of the resultant charging probabilities into the computer codes for EMI susceptability then allow an evaluation of arcing consequences.

4) External arc sources can be used to experimentally simulate the EMI effects of vacuum arcs.

To date, no attempt has been made to develop a test procedure for spacecraft to simulate the arcing problem. However, such a test is planned in the near future at TRW in which an operation spacecraft will be irradiated by energetic electron beams (A. Rosen Private Communication). However, it was the general consensus of opinion at both TRW (F. Scarf and A. Rosen) and the Aerospace Corp. (R. Holzworth and J. M. Cornwall) that this planned test is unique and that routine similar spacecraft testing to evaluate charging effects would not be an operation requirement for future GEO flights.

References

Bernstein W, B Hultqvist and H Borg "Some duplications of low altitude observations of isotropic precipitation of ring current protons beyond the plasmapause" Planet. Space Sci., 22, 767-776, 1974.

Bernstein W, H Lembach, P J Kellogg, S J Monson and T Hallinan "Further laboratory measurements of beam-plasma discharge" J. Geophys. Res., 84, 7271-7278, 1979.

Bernstein W, B A Whalen, F R Harris, A G McNamara and A Konradi "Laboratory studies of the charge neutralization of a rocket payload during electron beam emissions" Geophys. Res. Lett., 7, 93-96, 1980.

Block L P "Interpretation of Laboratory Experiments of Interest to Space Physics" in Physics of Solar Planetary Environments, D J Williams, editor, American Geophysical Union, 1976.

Chappell C R "Recent satellite measurements of the morphology and dynamics of the plasmapause" Rev. Geophys. & Space Phys., 10, 951-981, 1972.

Cornwall J M, F V Coroniti and R M Thorne "A unified theory of SAR arc formation at the plasmapause" J. Geophys. Res., 76, 4428, 1970.

DeForest S E "Detection of the solar wind at synchronous orbit" J. Geophys. Res., 78, 1195, 1973.

DeForest S E "The plasma environment at geosynchronous orbit" in Proceedings of the Spacecraft Charging Technology Conference, C P Pike and R R Lovell, editors, AFGL-TR-77-0051, NASA TMX-73537, 1977.

Galeev A A, E V Mishin, R Z Sagdeev, V D Shapiro and V I Shevchenko "Discharge in the region around a rocket following injection of electron beams into the ionosphere" Sov. Phys. Doklady, 21, 641, 1976.

Garrett H B "Review of quantitative models of the 0 to 100 keV near-Earth plasma" Revs. Geophys. and Space Sci., 17, 397-418, 1979.

Ikegami H, H Ikeyi, T Kawamura, H Nomota, K Takagama and Y Terashima "Characteristics of microinstabilities in a hot electron plasma" Plasma Phys. & Controlled Nuclear Fusion Res., 2, 423, 1969.

Jacquinot J, C Leloup, J P Paffe, M de Pretis, F Waelbroch, P Evard and J Ripault "Etude des microinstabilites dans un plasma d'electrons chaude confines" Plasma Phys. & Controlled Nuclear Fusion Res., 2, 347, 1969.

Katz I, D E Parks, S Wang and A Wilson "Dynamics Modeling of Spacecraft in a Collisionless Plasma" in Proceedings of the Spacecraft Charging Technology Conference, C R Pike and R R Lovell, editors, AFGL TR-77-0051, NASA TMX-73537, 1977.

Kennel C F and H E Petschek "Limit on stably trapped particle fluxes" J. Geophys. Res., 71, 1, 1966.

Kennel C F, F L Scarf, R W Fredricks, J H McGehee and F V Coroniti "VLF electric field observations in the magnetosphere" J. Geophys. Res., __, 6136, 1970.

McIlwain C E "Auroral electron beams near the magnetic equator" Nobel Symposium, Kuuna, Sweden, 1975.

Wall J A, E A Burke and A R Frederickson "Result of Literature Search on Dielectric Properties and Properties and Electron Interaction Phenomena Related to Spacecraft Charging" in Proceedings of the Spacecraft Charging Technology Conference, C R Pike and R R Lovell, editors, AFGL TR-77-0051, NASA TMX-73537, 1977.

Williams D J and L R Lyons "The proton ring current and its interaction with the plasmapause: storm recovery phase" J. Geophys. Res., 79, 4195, ? .

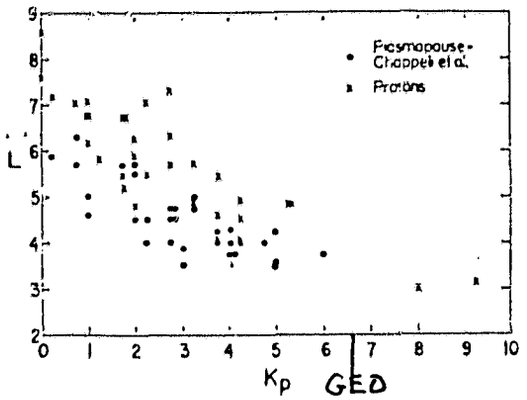

FIG. 2 DEPENDENCE OF THE LATITUDINAL LOCATION (L) OF THE POINT WHERE THE 6 keV PRECIPITATED (10°) PROTON FLUX FALLS BELOW THE DETECTION THRESHOLD ON GEOMAGNETIC ACTIVITY (K_p).

Also shown (·) are plasmapause locations determined by Chappell *et al.* (1970) for equivalent geomagnetic conditions.

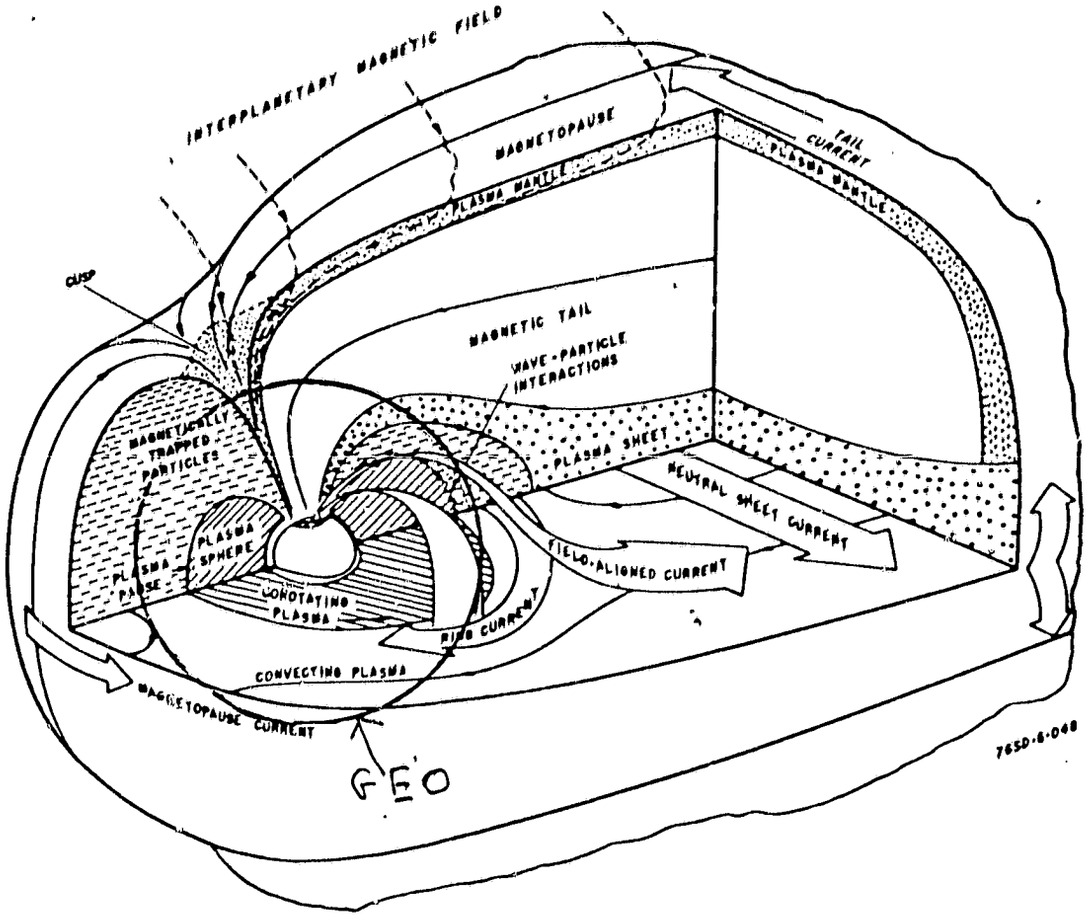

Figure 1. Magnetosphere (after Heikkila)

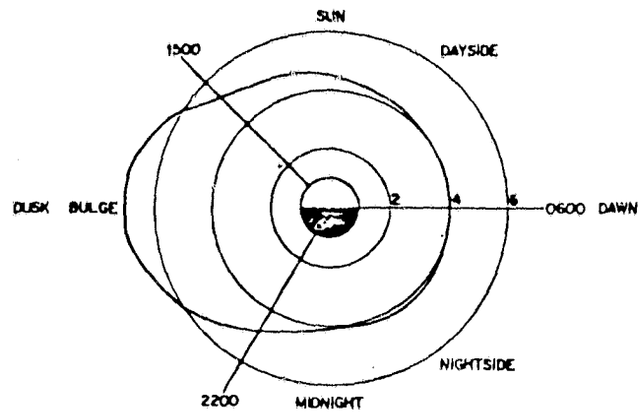

Fig. 3. An L, local-time plot showing the different local-time sectors of the plasmasphere (dayside, nightside, and bulge). The solid line shows the average plasmapause position determined from more than 150 Ogo 5 profiles [*Chappell et al.*, 1971*b*].